PAPER

Low Complexity Metric for Joint MLD in Overloaded MIMO System

Takayoshi AOKI[†a)], ***Student Member and*** **Yukitoshi SANADA**[†b)], ***Senior Member***

SUMMARY This paper presents a low complexity metric for joint maximum-likelihood detection (MLD) in overloaded multiple-input multiple-output (MIMO)-orthogonal frequency division multiplexing (OFDM) systems. In overloaded MIMO systems, a nonlinear detection scheme such as MLD combined with error correction coding achieves better performance than is possible with a single signal stream with higher order modulation. However, MLD incurs high computation complexity because of the multiplications in the selection of candidate signal points. Thus, a Manhattan metric has been used to reduce the complexity. Nevertheless, it is not accurate and causes performance degradation in overloaded MIMO systems. Thus, this paper proposes a new metric whose calculations involve only summations and bit shifts. New numerical results obtained through computer simulation show that the proposed metric improves bit error rate (BER) performance by more than 0.2 dB at the BER of 10^{-4} in comparison with a Manhattan metric.

key words: *overloaded MIMO, joint MLD*

1. Introduction

Recently, mobile phones and wireless local area networks (LANs) are widely used all over the world. Wireless communication systems have to accommodate a large amount of data traffic. Multiple-input multiple-output (MIMO) has been proposed to realize wireless communication systems with larger capacity and better reliability [1], [2]. MIMO uses multiple antenna elements at both the transmitter and receiver.

However, a limited number of receive antennas can be implemented in a mobile terminal owing to its form factor. Thus, overloaded MIMO has been investigated [3]. In overloaded MIMO systems there are fewer receive antenna elements than transmit antenna elements. In the receivers of overloaded MIMO systems, nonlinear detection schemes such as maximum likelihood detection (MLD) are applied in conjunction with error correction coding and it achieves superior performance as compared to a single signal stream with higher order modulation [4], [5]. However, the computational complexity of MLD increases exponentially with the number of signal streams. In order to decrease the detection complexity in overloaded MIMO systems, a linear detection scheme has been proposed [6]–[9]. In these literatures, virtual channels are created by transforming the complex channel and signal matrices to the real value matrices. With the combination of iterative detection and decoding, these schemes achieve better performance than that with MLD at the same time as realizing complexity reduction.

For the complexity reduction of MLD, on the other hand, QR decomposition and M-algorithm (QRM)-MLD and sphere decoding have also been applied to the overloaded MIMO-orthogonal frequency division multiplexing (OFDM) systems [10]–[12]. However, matrix computations are also required in these schemes to reduce the number of candidate signal points. In addition, these schemes need to calculate a Euclidean metric between a received signal point and candidate signal points though the number of the candidate points are limited. The Euclidean metric is derived through multiplications which greatly increases the computation complexity. A Manhattan metric has been proposed as a substitute of the Euclidean metric. However, the performance with the Manhattan metric in MLD is degraded [13]. The correlation metric has also been proposed in [13]. The correlation metric needs to calculate multiplications and the number of multiplications increases in proportion to the square of the number of the transmit antennas and to the number of the receive antennas.

This paper then proposes a low complexity metric that is calculated only through summations and bit shifts. The proposed metric uses the subtraction of the differences on the real and imaginary parts between a received signal point and a candidate signal constellation point as well as the sum of those differences. The numbers of multiplications per receive antenna with the proposed metric and the Manhattan metric are in proportion to the number of transmit signal streams while it increases exponentially in the Euclidean metric. On the other hand, the number of summations per receive antenna increases exponentially to the number of the signal streams in the calculation of all the metrics. The proposed metric realizes better approximation as compared to the Manhattan metric.

This paper is organized as follows. Section 2 describes the system model. Section 3 explains the simulation conditions. In Sect. 4, the numerical results obtained through computer simulation are presented. Section 5 gives our conclusions.

Manuscript received February 26, 2015.
Manuscript revised August 27, 2015.

[†]The authors are with the Dept. of Electronics and Electrical Engineering, Keio University, Yokohama-shi, 223-8521 Japan.
a) E-mail: takayoshiaoki@elec.keio.ac.jp
b) E-mail: sanada@elec.keio.ac.jp

DOI: 10.1587/transcom.2015EBP3082

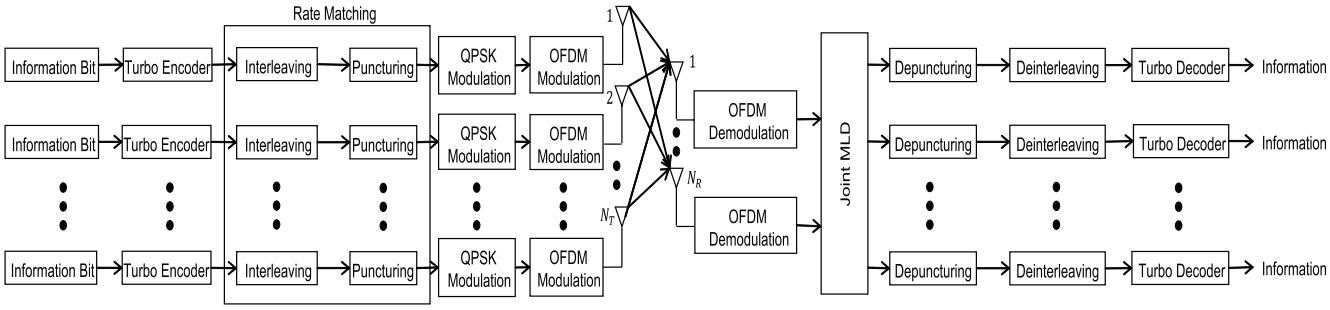

Fig. 1 Overloaded MIMO-OFDM system.

2. System Description

2.1 Signal Model

The block diagram of an overloaded MIMO-OFDM system with joint MLD is shown in Fig. 1. Information bits are encoded by the turbo code and the coded bits are rearranged by the interleaver. The code rate is then adjusted through puncturing in the rate matching block. After puncturing M coded bits are allocated to a 2^MQAM symbol. The symbol on the lth subcarrier, $S_p[l]$, is transmitted from the pth transmit antenna. The OFDM signal transmitted from the pth transmit antenna is given by

$$u_p[n] = \sum_{l=0}^{N-1} S_p[l] \exp\left(j\frac{2\pi nl}{N}\right) \tag{1}$$

where n is the time index ($n = 0, 1, ..., N-1$), N is the size of the inverse discrete Fourier transform (IDFT). A guard interval (GI) is then added by replicating the last part of the OFDM symbol. The transmit signal from the pth antenna is written as

$$v_p(t) = \sum_{n=-N_{GI}}^{N-1} u_p[n] p_{tp}(t - nT_s) \tag{2}$$

where $p_{tp}(t)$ is the impulse response of the transmit filter, T_s is the sampling interval of the OFDM symbol, and N_{GI} is the GI length. In the receiver side, the received signal at the qth receive antenna is given by

$$y_q(t) = \sum_{p=1}^{N_T} y_{qp}(t) + n_q(t) \tag{3}$$

where $n_q(t)$ is the noise at the qth receive antenna and $y_{qp}(t)$ is the received signal from the pth transmit antenna to the qth receive antenna. $y_{qp}(t)$ is calculated by

$$y_{qp}(t) = \sum_{n=-N_{GI}}^{N-1} u_p[n] h_{qp}(t - nT_s) \tag{4}$$

where $h_{qp}(t)$ is the impulse response of the channel between the pth transmit and qth receive antennas and it includes the transmit and receive filters. The received signal is converted to digital samples by an A/D converter at the rate of T_s. Therefore, the received digital signal is given as

$$y_q[n] = y_q(nT_s). \tag{5}$$

After removing the GI and taking the DFT of N samples, the signal on the lth subcarrier is expressed as

$$\begin{aligned} Y_q[l] &= \sum_{n=0}^{N-1} y_q[n] \exp\left(j\frac{-2\pi nl}{N}\right) \\ &= \sum_{p=1}^{N_T} H_{qp}[l] S_p[l] + N_q[l] \end{aligned} \tag{6}$$

where $H_{qp}[l]$ is the frequency response between the pth transmit antenna and the qth receive antenna and $N_q[l]$ is the noise through the qth receive antenna on the lth subcarrier. It can be written in a matrix form as

$$\mathbf{Y}[l] = \mathbf{H}[l]\mathbf{S}[l] + \mathbf{N}[l] \tag{7}$$

where

$$\mathbf{Y}[l] = [Y_1[l]\ Y_2[l]\ \ldots\ Y_{N_R}[l]]^T, \tag{8}$$

$$\mathbf{H}[l] = \begin{bmatrix} H_{11}[l] & \cdots & H_{1N_T}[l] \\ \vdots & \ddots & \vdots \\ H_{N_R1}[l] & \cdots & H_{N_RN_T}[l] \end{bmatrix}, \tag{9}$$

$$\mathbf{S}[l] = [S_1[l]\ S_2[l]\ \ldots\ S_{N_T}[l]]^T, \tag{10}$$

$$\mathbf{N}[l] = [N_1[l]\ N_2[l]\ \ldots\ N_{N_R}[l]]^T. \tag{11}$$

2.2 Calculation the LLR for Joint MLD

A log-likelihood ratio (LLR) is calculated for each coded bit in the systematic part of the codeward in joint MLD. The likelihood values for the mth bit of the symbol in the pth signal are given as follows;

$$D^1_{pm} = \sum_{\hat{\mathbf{S}}^1_{pm} \in \{\mathbf{S}\} b_{pm}=1} \exp\left(-\tfrac{1}{\sigma^2}\|\mathbf{Y}[l] - \mathbf{H}[l]\hat{\mathbf{S}}^1_{pm}\|^2\right), \tag{12}$$

$$D^0_{pm} = \sum_{\hat{\mathbf{S}}^0_{pm} \in \{\mathbf{S}\} b_{pm}=0} \exp\left(-\tfrac{1}{\sigma^2}\|\mathbf{Y}[l] - \mathbf{H}[l]\hat{\mathbf{S}}^0_{pm}\|^2\right), \tag{13}$$

where σ^2 is the noise variance, $\hat{\mathbf{S}}^1_{pm}$ or $\hat{\mathbf{S}}^0_{pm}$ is the vector

of candidate N_T symbols in which the mth coded bit of a 2^MQAM symbol from the pth transmit antenna is "1" or "0", $\mathbf{S} = [S_1\ S_2\ \ldots\ S_{N_T}]^T$ is the candidate symbol vector, $\{\mathbf{S}\}_{b_{pm}=1}$ or $\{\mathbf{S}\}_{b_{pm}=0}$ is the set of the symbol vectors in which the mth coded bit of the pth 2^MQAM symbol, S_p, is "1" or "0", and D^1_{pm} or D^0_{pm} is the sum of the likelihood values for the mth coded bit of "1" or "0" in the pth symbol, respectively. The LLR is calculated as,

$$L(b_{pm}|\mathbf{Y}[l]) = \log \frac{D^1_{pm}}{D^0_{pm}} \tag{14}$$

where $L(b_{pm}|\mathbf{Y}[l])$ is the LLR of the mth bit of the symbols on the lth subcarrier transmitted from the pth antenna.

2.3 Approximation of LLR

The approximation of the LLR with the dominant terms has been given in [14]. The approximated LLR is given as

$$\begin{aligned} L(b_{pm}|\mathbf{Y}[l]) \approx (-\tfrac{1}{\sigma^2}\|\mathbf{Y}[l]-\mathbf{H}[l]\overline{\mathbf{S}}^1_{pm}\|^2) \\ -(-\tfrac{1}{\sigma^2}\|\mathbf{Y}[l]-\mathbf{H}[l]\overline{\mathbf{S}}^0_{pm}\|^2) \end{aligned} \tag{15}$$

where $\overline{\mathbf{S}}^1_{pm}$ or $\overline{\mathbf{S}}^0_{pm}$ is one of the candidate symbol vectors in $\{\hat{\mathbf{S}}^1_{pm}\}$ or $\{\hat{\mathbf{S}}^0_{pm}\}$ and it gives the minimum Euclidean metric from $\mathbf{Y}[l]$ as follows;

$$\overline{\mathbf{S}}^1_{pm} = \underset{\hat{\mathbf{S}}^1_{pm}\in\{\mathbf{S}\}_{b_{pm}=1}}{\arg\min} \sum_{q=1}^{N_R}\{(\Re[E^1_{qpm}[l]])^2 + (\Im[E^1_{qpm}[l]])^2\}, \tag{16}$$

$$\overline{\mathbf{S}}^0_{pm} = \underset{\hat{\mathbf{S}}^0_{pm}\in\{\mathbf{S}\}_{b_{pm}=0}}{\arg\min} \sum_{q=1}^{N_R}\{(\Re[E^0_{qpm}[l]])^2 + (\Im[E^0_{qpm}[l]])^2\}, \tag{17}$$

where $E^1_{qpm}[l]$ or $E^0_{qpm}[l]$ is the difference between the coordinates of the received signal and the candidate signal point in which the mth coded bit of the pth signal stream is "1" or "0" and these are calculated by the followings;

$$E^1_{qpm}[l] = Y^1_q[l] - \mathbf{H}^1_{qp}[l]\hat{\mathbf{S}}^1_{pm}[l], \tag{18}$$

$$E^0_{qpm}[l] = Y^0_q[l] - \mathbf{H}^0_{qp}[l]\hat{\mathbf{S}}^0_{pm}[l], \tag{19}$$

where $\mathbf{H}_{qp}[l] = \left[H_{q1}[l]\ H_{q2}[l]\ \ldots\ H_{qN_T}[l]\right]^T$.

This approximation omits the calculation of exponential terms. However, it is required to determine the dominant terms by calculating the Euclidean metric.

2.4 Metric Calculation without Multiplication

2.4.1 Conventional Metric

In the joint MLD, the metrics between the received signal and all the candidate signal points are required to be calculated. It is necessary to calculate the Euclidean metrics for all the combinations of the encoded symbols from the N_T signal streams. The number of multiplications increase exponentially with the number of signal streams. In order to reduce the complexity, a Manhattan metric has been introduced in MLD [13].

The Manhattan metric between the received signal and the candidate signal points are calculated and the candidate symbol vector with the minimum among them is selected as follows;

$$\tilde{\mathbf{S}}^{c1}_{pm} = \underset{\hat{\mathbf{S}}^1_{pm}\in\{\mathbf{S}\}_{b_{pm}=1}}{\arg\min} \sum_{q=1}^{N_R}(|\Re[E^1_{qpm}[l]]| + |\Im[E^1_{qpm}[l]]|), \tag{20}$$

$$\tilde{\mathbf{S}}^{c0}_{pm} = \underset{\hat{\mathbf{S}}^0_{pm}\in\{\mathbf{S}\}_{b_{pm}=0}}{\arg\min} \sum_{q=1}^{N_R}(|\Re[E^0_{qpm}[l]]| + |\Im[E^0_{qpm}[l]]|), \tag{21}$$

where $\tilde{\mathbf{S}}^{c1}_{pm}$ or $\tilde{\mathbf{S}}^{c0}_{pm}$ is the candidate symbol vector from $\{\hat{\mathbf{S}}^1_{pm}\}$ or $\{\hat{\mathbf{S}}^0_{pm}\}$ with the smallest Manhattan metric, and $E^1_{qpm}[l]$ and $E^0_{qpm}[l]$ are calculated by Eqs. (18) and (19). The approximated LLR is calculated with the following equations.

$$\tilde{D}^1_{pm} = \frac{1}{\sigma^2}\|\mathbf{Y}[l] - \mathbf{H}[l]\tilde{\mathbf{S}}^1_{pm}\|^2, \tag{22}$$

$$\tilde{D}^0_{pm} = \frac{1}{\sigma^2}\|\mathbf{Y}[l] - \mathbf{H}[l]\tilde{\mathbf{S}}^0_{pm}\|^2, \tag{23}$$

$$L(b_{pm}|\mathbf{Y}[l]) \approx \tilde{D}^1_{pm} - \tilde{D}^0_{pm}. \tag{24}$$

2.4.2 Proposed Metric

The proposed metric consists of the two terms, $\|\Re[E^*_{qpm}]| + |\Im[E^*_{qpm}]\|$ and $\|\Re[E^*_{qpm}] - \Im[E^*_{qpm}]\|$ ($* =$ "1" or "0"), for the selection of the candidate signal vector among $\{\hat{\mathbf{S}}^1_{pm}\}$ or $\{\hat{\mathbf{S}}^0_{pm}\}$. These terms are combined with corresponding coefficients. The curves of the metrics are drawn when the difference of the coordinates of the signal points is given as $e^{i\theta}$ when θ is from 0 to $\pi/2$ in Fig. 2. Here, the Euclidean metric is constant and its value is normalized to $|e^{i\theta}| = 1$. For the same difference of the coordinates, the Manhattan metric shows the maximum value of 1.41 at $\theta = \pi/4$. The proposed metric achieves a smaller error from the Euclidean metric than that of the Manhattan metric.

The candidate symbol vector with the minimum metric is selected as the following equations.

$$\begin{aligned} \tilde{\mathbf{S}}^{n1}_{pm} = \underset{\hat{\mathbf{S}}^1_{pm}\in\{\mathbf{S}\}_{b_{pm}=1}}{\arg\min} \sum_{q=1}^{N_R}\{C_+(|\Re[E^1_{qpm}[l]]| + |\Im[E^1_{qpm}[l]]|) \\ +C_-(\|\Re[E^1_{qpm}[l]]| - |\Im[E^1_{qpm}[l]]\|)\}, \end{aligned} \tag{25}$$

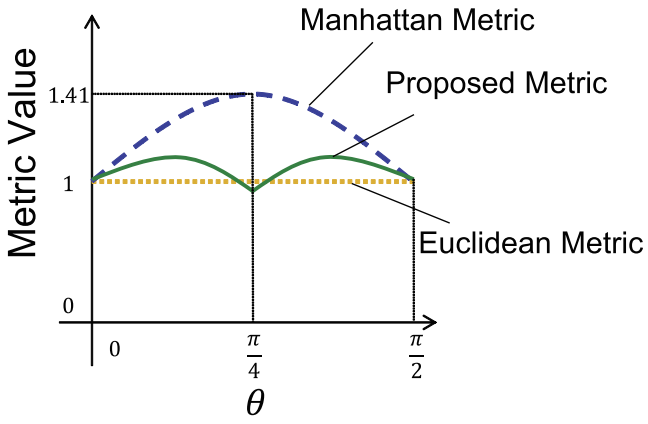

Fig. 2 Conventional and proposed metrics.

$$\tilde{\mathbf{S}}_{pm}^{n0} = \underset{\hat{\mathbf{S}}_{pm}^{0} \in \{\mathbf{S}\}_{b_{pm}=0}}{\arg\min} \sum_{q=1}^{N_R} \{C_+(|\Re[E_{qpm}^{0}[l]]| + |\Im[E_{qpm}^{0}[l]]|) + C_-(||\Re[E_{qpm}^{0}[l]]| - |\Im[E_{qpm}^{0}[l]]||)\}, \tag{26}$$

where $\tilde{\mathbf{S}}_{pm}^{n1}$ or $\tilde{\mathbf{S}}_{pm}^{n0}$ is the candidate symbol vector from $\{\hat{\mathbf{S}}_{pm}^{1}\}$ or $\{\hat{\mathbf{S}}_{pm}^{0}\}$ with the smallest metric, $E_{qpm}^{1}[l]$ and $E_{qpm}^{0}[l]$ are calculated by Eqs. (18) and (19), and C_+ and C_- are the coefficients that decide the ratio of the two terms, $||\Re[E_{qpm}^{*}]| + |\Im[E_{qpm}^{*}]||$ and $||\Re[E_{qpm}^{*}] - \Im[E_{qpm}^{*}]||$. For the reduction of the computationally complexity, C_+ and C_- are given with the following condition.

$$C_+ = 1 - C_- = \sum_k \frac{C_k}{2^k} \tag{27}$$

where k is an integer and $C_k = \{-1, 0, 1\}$. It is then possible to substitute the multiplication of the coefficient through bit shifts and summations. With the selected candidate symbol vectors the likelihood ratio is then calculated by Eq. (15).

3. Numerical Results

3.1 Simulation Conditions

The simulation conditions are shown in Table 1. A turbo code with 8 state memory is applied as the error-correction code [15]. The base rate of the code is 1/3 and the code rate is selected from 1/3, 1/2, 5/6 through puncturing. The interleaver size is fixed to 4800. The number of the transmit antennas is selected from 2 to 4 while the number of the receive antennas is fixed to 2. Each signal stream is modulated with QPSK, 16QAM, 64QAM and multiplexed through OFDM. The channel bandwidth is 2.5 MHz and subcarrier spacing is 15 kHz. The number of subcarriers is 256 while the number of data subcarriers is 151. The sampling frequency is then 3.84 MHz. The guard interval of the 1st symbol is 5.21 μs, and the 2nd-7th symbols are 4.69 μs. 6 Taps GSM-TU is assumed as a channel model [16]. Channel estimation in the receiver is assumed to be ideal. The decoding algorithm is log-MAP and the number of decoding iterations is 8. For each plot, 9.6×10^6 bits are transmitted.

Table 1 Simulation conditions.

Error Correction Coding	Turbo Code
Code Rate	1/3, 1/2, 5/6
Interleave Size	4800
Modulation Scheme	QPSK,16QAM,64QAM /OFDM
Number of Signal Streams	2~4
Number of Transmit Antennas	2~4
Number of Receive Antennas	2
Channel Bandwidth	2.5 MHz
Subcarrier Spacing	15 kHz
Number of Subcarriers	256
Number of Data Subcarriers	151
Sampling Frequency	3.84 MHz
Guard Interval	5.21 μs (1st symbol) 4.69 μs (2nd-7th symbols)
Decoding Algorithm	Log-MAP
Number of Decoding Iterations	8
Channel Model	6 Taps GSM-TU
Channel Estimation	Ideal
Scheme I : $(C_+, C-)$ Scheme II : $(C_+, C-)$ Scheme III : $(C_+, C-)$ Scheme IV : $(C_+, C-)$	$(\frac{21}{32}, \frac{11}{32})$ $(\frac{11}{16}, \frac{5}{16})$ $(\frac{5}{8}, \frac{3}{8})$ $(2, 1)$
Number of Bits	9.6×10^6

3.2 Coefficients of Proposed Metric

The coefficients for the proposed metric are selected from $(C_+, C-) = (\frac{21}{32}, \frac{11}{32}), (\frac{11}{16}, \frac{5}{16}), (\frac{5}{8}, \frac{3}{8}), (2, 1)$. They are referred to as the proposed scheme I, II, III, and IV. These sets of the coefficients for the proposed metric I, II, and III correspond to the maximum value of k in Eq. (27). The coefficients for the proposed metric I, II, and III are calculated with k of up to 5, 4, and 3. The coefficients, $\{C_k\}$, are selected so that the resultant metric is close to the Euclidean metric with respect to the mean error. The metrics for the maximum k of 1 and 2 are excluded since they are not close to the Euclidean metric than the proposed metrics in terms of the parameters shown in Table 2. As for the metrics with the maximum k of more than 6 are also excluded since they require more bit shifts and summations that lead to larger complexity. The coefficients of $(C_+, C_-) = (2, 1)$ are selected for its simplicity as it requires only one bit shift though they do not satisfy the condition of $C_+ = 1 - C_-$. The curves of the proposed metrics are presented in Fig. 3. For the case of the proposed scheme IV, the coefficients of $\frac{1}{3}(2, 1)$ are used to draw the curve though 1/3 is omitted at the selection of the candidate signal point for complexity reduction. The mean, the mean square, and the maximum difference from the Euclidean metric is shown in Table 2. It is clear that the mean and the maximum of the errors with the proposed metric are smaller than those of the Manhattan metric.

Table 2 Accuracy of metrics.

Method	Mean	Mean Square	Max.
Manhattan Metric	0.2716	0.0896	0.4142
Proposed Metric I	0.0319	0.0013	0.0697
Proposed Metric II	0.0422	0.0023	0.0680
Proposed Metric III	0.0318	0.0017	0.1137
Proposed Metric IV	0.0342	0.0014	0.0550

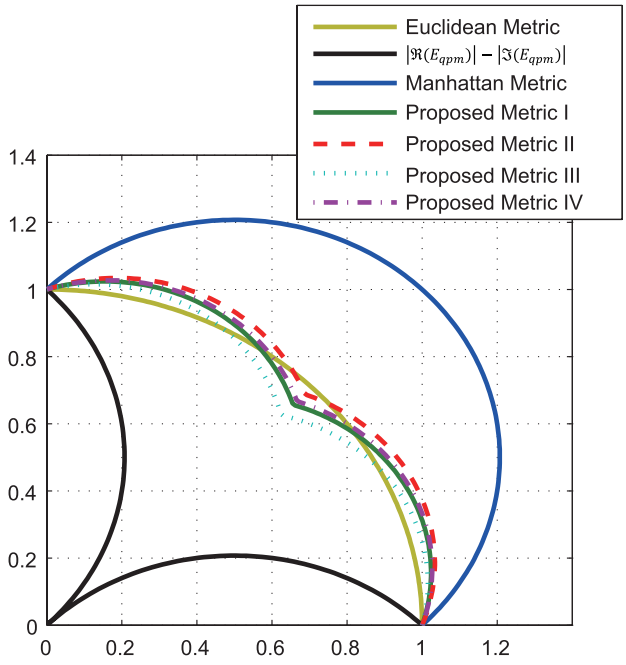

Fig. 3 Curves of proposed metric I, II, III, IV.

3.3 BER Performance

The bit error rate (BER) versus E_b/N_0 with 3 signal streams for the code rates of 1/3, 1/2, and 5/6 on the 6 Taps GSM-TU channel is shown in Figs. 4–6, respectively. The performance with the LLR approximation deteriorates by 0.4 dB in Fig. 4, by 0.2 dB in Fig. 5, and by 0.05 dB in Fig. 6 at the BER of 10^{-4} as compared to that without approximation. The BER with the Manhattan metric further increases the required E_b/N_0 by 0.2–0.4 dB. On the other hand, the proposed metric improves the BER performance by more than 0.2 dB in Fig. 4, 0.2 dB in Fig. 5, and 0.05 dB in Fig. 6 at the BER of 10^{-4} in comparison with the Manhattan metric.

The required E_b/N_0 at BER=10^{-4} versus the code rate with 3 signal streams on the 6 Taps GSM-TU channel is shown in Fig. 7. It is shown that the amount of the degradation on the required E_b/N_0 reduces as the code rate grows in Fig. 7. This is because the error-correcting capability of the turbo decode deteriorates as the code rate increases. The proposed metrics I, II, IV are relatively better than the proposed metric III because the maximum difference is smaller.

The required E_b/N_0 at BER=10^{-4} versus the number of signal streams with the code rate of 1/3 on the 6 Taps GSM-TU channel is shown in Fig. 8. It is shown that the amount of

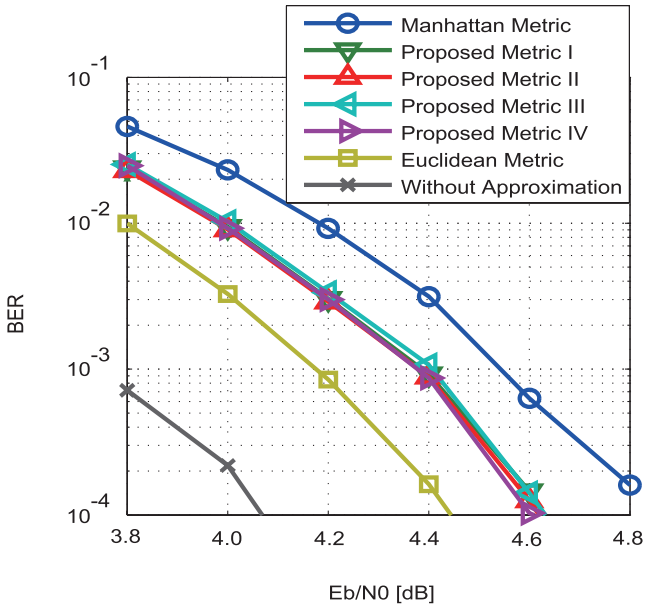

Fig. 4 BER vs. E_b/N_0 (3 signal streams, code rate of 1/3, QPSK, 6 Taps GSM-TU).

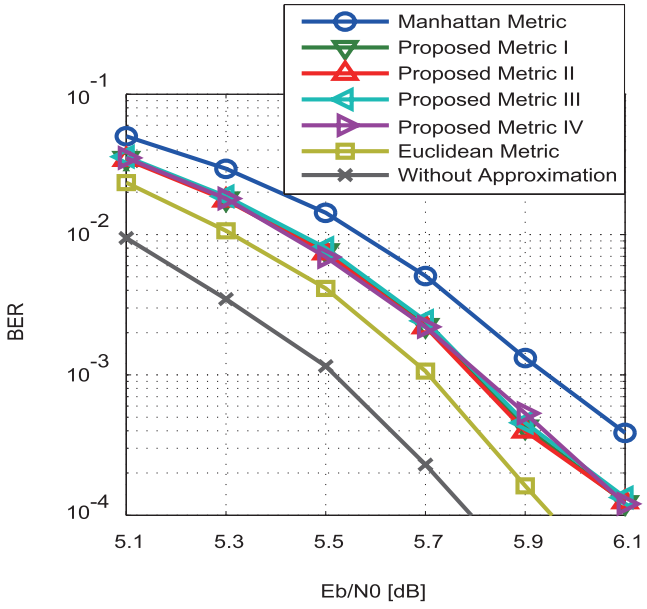

Fig. 5 BER vs. E_b/N_0 (3 signal streams, code rate of 1/2, QPSK, 6 Taps GSM-TU).

the performance degradation with the LLR approximations enlarges as compared to that without approximation when the number of signal streams increases. The reason is that the error of the metric causes the miss selection of the candidate signal point more often as the number of signal streams increases. The proposed metrics achieve closer performance to that with the Euclidean metric than the Manhattan metric when the number of signal streams is up to 4.

The BER curves versus E_b/N_0 with 3 signal streams with 16QAM or 64QAM are shown in Figs. 9 and 10, respectively. The code rate is set to 1/2. It is clear that the

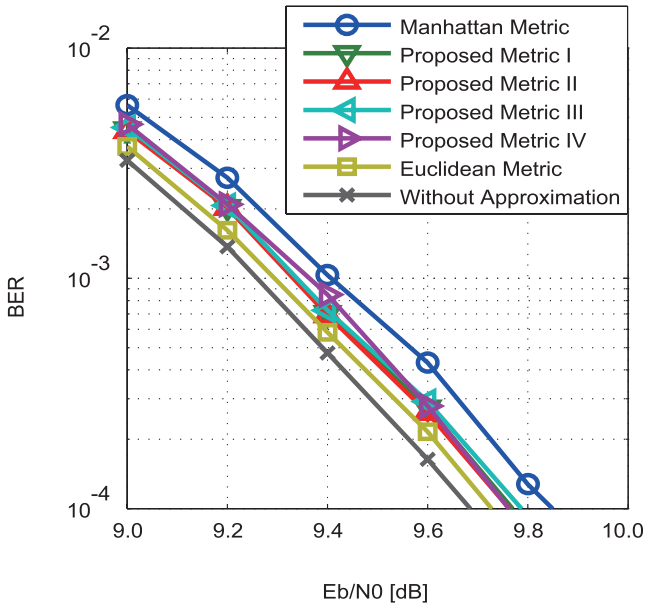

Fig. 6 BER vs. E_b/N_0 (3 signal streams, code rate of 5/6, QPSK, 6 Taps GSM-TU).

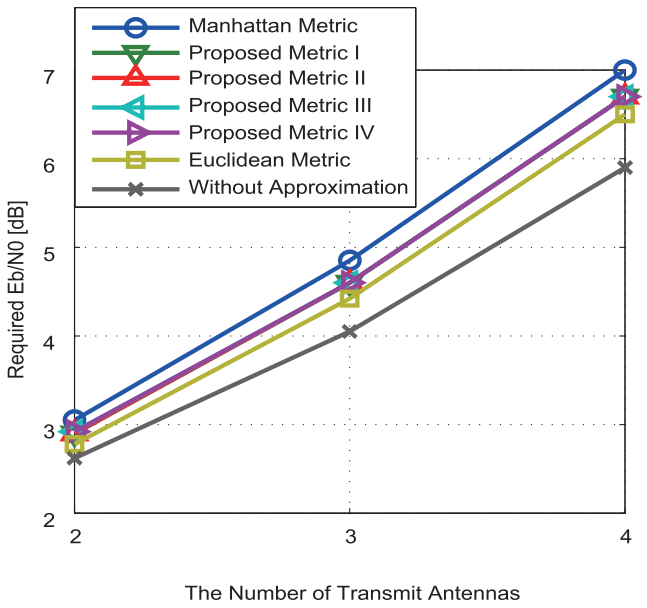

Fig. 8 Required E_b/N_0 at BER=10^{-4} vs. number of signal streams (code rate of 1/3, QPSK, 6 Taps GSM-TU).

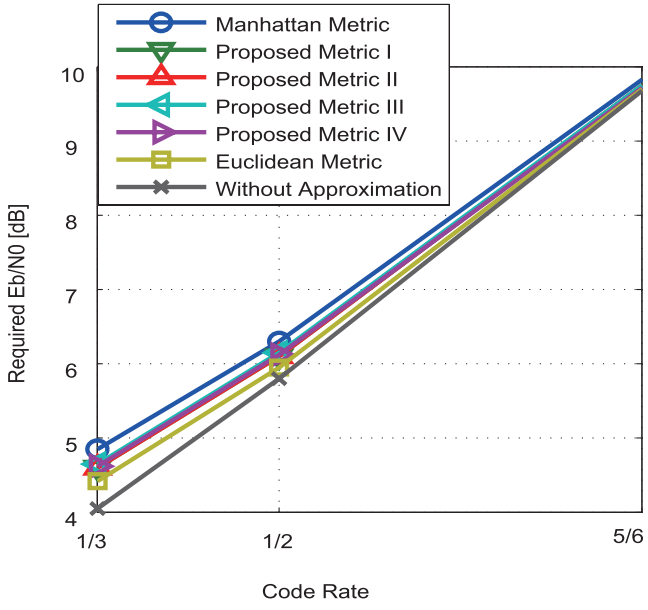

Fig. 7 Required E_b/N_0 for BER=10^{-4} vs. code rate (3 signal streams, QPSK, 6 Taps GSM-TU).

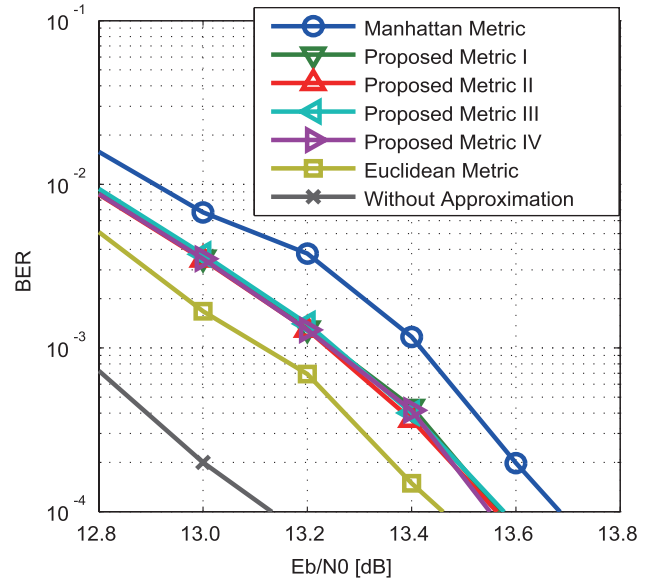

Fig. 9 BER vs. E_b/N_0 (3 signal streams, code rate of 1/2, 16QAM, 6 Taps GSM-TU).

performance with 16QAM and 64QAM shows the similar tendency as that with QPSK modulation in Fig. 5. The performance improvements with the proposed metric are about 0.1 dB as compared to those with the Manhattan metric in both Figs. 9 and 10.

3.4 Complexity

The numbers of multiplications, summations, and bit shifts for each metric are shown in Table 3. The numbers of multiplications in the proposed metrics and the Manhattan metric per receive antenna are in proportion to the number of transmit signal streams while it increases exponentially in the Euclidean metric. On the other hand, the numbers of summations per receive antenna increase exponentially to the number of the signal streams in all the metrics. The proposed metric requires from 5/3 to 3 times of summations as compared to the Manhattan metric. The proposed metric also needs additional bit shift operations though their complexity is independent of the number of signal streams.

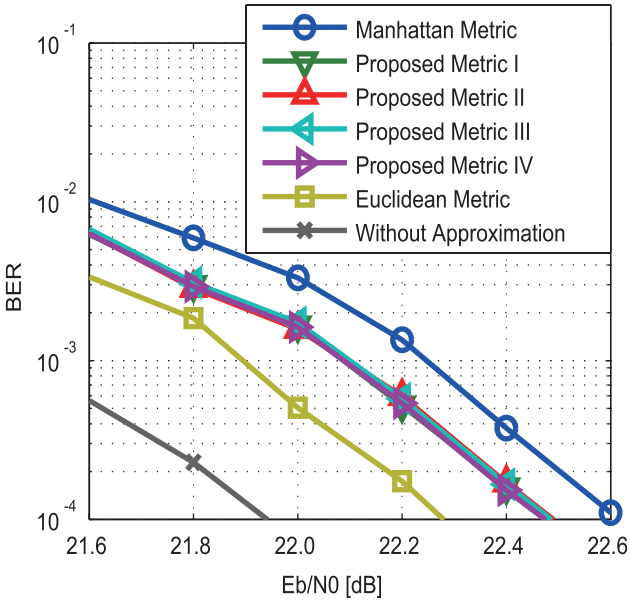

Fig. 10 BER vs. E_b/N_0 (3 signal streams, code rate of 1/2, 64QAM, 6 Taps GSM-TU).

Table 3 Complexity of metrics.

Method	Multiplications	Summations	Bit Shifts
Euclidean Metric	$2^{2N_T}N_R$	$2^{2N_T}N_R$	0
Manhattan Metric	$2\times 2N_TN_R$	$3\times 2^{2N_T}N_R$	0
Proposed Metric I	$2\times 2N_TN_R$	$9\times 2^{2N_T}N_R$	$6N_R$
Proposed Metric II	$2\times 2N_TN_R$	$8\times 2^{2N_T}N_R$	$4N_R$
Proposed Metric III	$2\times 2N_TN_R$	$7\times 2^{2N_T}N_R$	$4N_R$
Proposed Metric IV	$2\times 2N_TN_R$	$5\times 2^{2N_T}N_R$	N_R

4. Conclusions

This paper proposes a low complexity metric that is calculated only through summations and bit shifts. The proposed metric uses the subtraction of the differences on the real and imaginary parts between a received signal point and a candidate signal constellation point as well as the sum of those differences.

The numerical results obtained through computer simulation show that the proposed metric improves the BER performance by more than 0.2 dB at the BER of 10^{-4} in comparison with that with the Manhattan metric. The performance degradation with the proposed metric is enhanced at low code rates while it is almost the same performance as that without approximation with the higher code rate. The proposed metric achieves better performance than that with the Manhattan metric even though the number of signal streams increases.

Acknowledgments

This work is supported in part by Ministry of Internal Affairs and Communications in Japan under the project name of Strategic Information and Communications R&D Promotion Programme (SCOPE 141303004).

References

[1] G.J. Foschini, "Layered space-time architecture for wireless communication in a fading environment when using multi-element antennas," Bell Labs Tech. J., vol.1, no.2, pp.41–59, 1996.
[2] G.J. Foschini and M.J. Gans, "On limits of wireless communications in a fading environment when using multiple antennas," Wireless. Pers. Commun., vol.6, no.3, pp.311–335, March 1998.
[3] S.J. Grant and J.K. Cavers, "Performance enhancement through joint detection of cochannel signals using diversity arrays," IEEE Trans. Commun., vol.46, no.8, pp.1038–1049, Aug. 1998.
[4] H. Murata and S. Yoshida, "Trellis-coded cochannel interference canceller for microcellular radio," IEEE Trans. Commun., vol.45, no.9, pp.1088–1094, Sept. 1997.
[5] Y. Sanada, "Performance of joint maximum-likelihood decoding for block coded signal streams in overloaded MIMO-OFDM system," 2013 International Symposium on Intelligent Signal Processing and Communication Systems, pp.775–780, 2013.
[6] S. Denno, H. Maruyama, D. Umehara, and M. Morikura, "A virtual layered space time receiver with maximum likelihood channel detection," Proc. IEEE 69th Vehicular Technology Conference, VTC Spring 2009, pp.1–5, 2009.
[7] S. Yoshikawa, S. Denno, and M. Morikura, "Complexity reduced lattice-reduction-aided MIMO receiver with virtual channel detection," IEICE Trans. Commun., vol.E96-B, no.1, pp.263–270, Jan. 2013.
[8] J. Imamura, S. Denno, D. Umehara, and M. Morikura, "A virtual layered space-frequency receiver architecture with iterative decoding," IEICE Trans. Commun., vol.E94-B, no.7, pp.1994–2002, July 2011.
[9] A. Taya, S. Denno, K. Yamamoto, M. Morikura, D. Umehara, H. Murata, and S. Yoshida, "An iterative MIMO receiver employing virtual channels with a turbo decoder for OFDM wireless systems," IEICE Trans. Commun., vol.E98-B, no.5, pp.878–889, May 2015.
[10] K.J. Kim, J. Yue, R.A. Iltis, and J.D. Gibson, "A QRD-M/Kalman filter-based detection and channel estimation algorithm for MIMO-OFDM systems," IEEE Trans. Wireless Commun., vol.4, no.2, pp.710–721, March 2005.
[11] H. Matsuoka, Y. Doi, T. Yabe and Y. Sanada, "Performance of overloaded MIMO-OFDM system with repetition code," 2014 International Symposium on Intelligent Signal Processing and Communication Systems, pp.239–244, 2014.
[12] I. Shubhi and Y. Sanada, "Trellis coded modulation with pseudo distance in overloaded MIMO OFDM with sphere decoding," 2013 International Symposium on Intelligent Signal Processing and Communication Systems, pp.579–584, 2013.
[13] T. Koike, Y. Seki, H. Murata, S. Yoshida, K. Araki, "Prototype implementation of real-time ML detectors for spatial multiplexing transmission," IEICE Trans. Commun., vol.E89-B, no.3, pp.845–852, March 2006.
[14] A.J. Viterbi, "An intuitive justification and a simplified implementation of the MAP decoder for convolutional codes," IEEE J. Sel. Areas. Commun., vol.16, no.2, pp.260–264, Feb. 1998.
[15] Multiplexing and channel coding, 3GPP TS 36.212 V11.4.0, Jan. 2014.
[16] Radio transmission and reception, 3GPP TS 45.005 V11.4.0, Jan. 2014.

Takayoshi Aoki was born in Fukuoka, Japan in 1992. He received his B.E. degree in electronics engineering from Keio University, Japan in 2015. Since April 2015, he has been a graduate student in School of Integrated Design Engineering, Graduate School of Science and Technology, Keio University. His research interests are mainly concentrates on MIMO-OFDM system.

Yukitoshi Sanada was born in Tokyo in 1969. He received his B.E. degree in electrical engineering from Keio University, Yokohama, Japan, his M.A.Sc. degree in electrical engineering from the University of Victoria, B.C., Canada, and his Ph.D. degree in electrical engineering from Keio University, Yokohama, Japan, in 1992, 1995, and 1997, respectively. In 1997 he joined the Faculty of Engineering, Tokyo Institute of Technology as a Research Associate. In 2000, he joined Advanced Telecommunication Laboratory, Sony Computer Science Laboratories, Inc, as an associate researcher. In 2001, he joined the Faculty of Science and Engineering, Keio University, where he is now a professor. He received the Young Engineer Award from IEICE Japan in 1997. His current research interests are in software defined radio, cognitive radio, and OFDM systems.